

**Syntheses of the Complete Set of Isomerically Pure,
Partially Fluorinated Cyclopentadienyl Ligands
(C₅F_{5-n}H_n) [n = 1–4] by Flash Vacuum Thermolysis of
(η^5 -Oxocyclohexadienyl)ruthenium Complexes.
Molecular Structures of [Ru(η^5 -C₅Me₅)(η^5 -C₅-1,2-F₂H₃)]
and [Ru(η^5 -C₅Me₅)(η^5 -C₅H₄F)]**

Russell P. Hughes,* Xiaoming Zheng, Christopher A. Morse,
Owen J. Curnow, and Jeffrey R. Lomprey

*Department of Chemistry, Burke Laboratory, Dartmouth College,
Hanover, New Hampshire 03755-3564*

Arnold L. Rheingold and Glenn P. A. Yap

Department of Chemistry, University of Delaware, Newark, Delaware 19716

Received September 2, 1997

A series of partially fluorinated (pentamethylcyclopentadienyl)(η^5 -oxocyclohexadienyl)-ruthenium complexes [RuCp*(2-6- η^5 -C₅F_{5-n}H_nCO)] (n = 1–4; Cp* = C₅Me₅) has been prepared by treatment of the cation [RuCp*(MeCN)₃]⁺ with thallium(I) salts of the corresponding phenols. Depending upon the number and location of the fluorine substituents, the complexes hydrogen bond to one-half of a molecule, one molecule, or no molecules of water. Subjection of these compounds to flash vacuum thermolysis (FVT) results in extrusion of CO and selective formation of the corresponding complexes [RuCp*(η^5 -C₅F_{5-n}H_n)] containing the monofluorocyclopentadienyl, 1,2-difluorocyclopentadienyl, 1,3-difluorocyclopentadienyl, 1,2,3-trifluorocyclopentadienyl, 1,2,4-trifluorocyclopentadienyl, and tetrafluorocyclopentadienyl ligands. ¹H, ¹⁹F, and ¹³C NMR spectra are reported for the new cyclopentadienyl ligands, and the ¹³C–¹⁹F coupling constants thus obtained are used to generate a full simulation of the ¹³C NMR spectrum of the pentafluorocyclopentadienyl ligand in [Ru(C₅Me₅)(C₅F₅)]. The solid-state structures of two complexes containing partially fluorinated cyclopentadienyl complexes have been determined by X-ray crystallography: [RuCp*(η^5 -C₅-1,2-F₂H₃)] (**15**), and [RuCp*(η^5 -C₅FH₄)] (**17**).

Introduction

For a number of years we have been interested in evaluating the effect of fluorine as a ligand substituent in transition-metal organometallic chemistry.¹ The σ -electron-withdrawing and π -electron-donating substituent effects of fluorine in organic molecules have been thoroughly examined and reviewed.² The chemical introduction of fluorine as a ligand substituent directly into organometallic systems has, in most cases, been unsuccessful, probably due to the strongly oxidizing conditions required, although one or two examples can be found in the literature. The first reported example, by Cais and Narkis, of a compound containing a fluorinated cyclopentadienyl ligand, [Mn(η^5 -C₅H₄F)(CO)₃], appeared in 1965.³ Introduction of fluorine was effected by a classical organic conversion of an amine substituent on the Cp ring to a diazonium salt followed

by decomposition of the BF₄ salt to afford the monofluorocyclopentadienyl ligand.³ However, the compound was characterized only by its IR spectrum, microanalysis for C, H, and Mn, and a melting point; no ¹H NMR and ¹⁹F NMR spectra were obtained. The relatively harsh conditions required for the conversion of the amino group on the Cp ring to a diazonium group severely limited the application of this synthetic method to the preparation of other fluorocyclopentadienyl complexes. The second example, monofluoroferrocene, was reported by Hedberg and Rosenberg,⁴ also by direct functionalization of a coordinated Cp ligand. Treatment of bromoferrocene with *n*-butyllithium gave lithioferrocene, which was then allowed to react with perchloryl fluoride gas in THF. The product, isolated in less than 10% yield, was identified as monofluoroferrocene by NMR and mass spectra. Alternatively, the same compound was obtained in 37% yield by Popov *et al.* in 1990 by reaction of trifluoroacetyl hypofluorite with mono-(acetoxymercuro)ferrocene.⁵ It is worth mentioning that while perchlorination of some metallocenes can be

(1) Hughes, R. P. *Adv. Organomet. Chem.* **1990**, *31*, 183.

(2) Smart, B. E. In *The Chemistry of Functional Groups, Supplement D* Patai, S., Rappoport, Z., Eds.; John Wiley & Sons: New York, 1983; Chapter 4. Smart, B. E. *Organofluorine Chemistry, Principles and Applications*; Banks, R. E., Smart, B. E., Tatlow, J. L., Eds; Plenum: New York, 1994; Chapter 3.

(3) Cais, M.; Narkis, N. *J. Organomet. Chem.* **1965**, *3*, 269.

(4) Hedberg, F. L.; Rosenberg, H. *J. Organomet. Chem.* **1971**, *28*, C14

(5) Popov, V. I.; Lib, M.; Hass, A. *Ukr. Khim. Zh.* **1990**, *56*, 1115.

similarly accomplished by mercuration followed by halogen substitution, analogous perfluorination of Cp ligands has not been accomplished.^{6–8}

In view of the challenges associated with the introduction of fluorine directly into organometallic molecules, we have limited our synthetic approaches to those which have all of the necessary carbon–fluorine bonds in place before complexation of the ligand. In the case of the perfluorocyclopentadienyl ligand, this posed a significant problem; although the $C_5F_5^-$ anion is known,⁹ attempts to use it as a precursor to transition-metal complexes proved to be frustratingly unsuccessful.¹⁰ Our eventual synthetic approach to fluorinated cyclopentadienyl ligands resulted from the realization that certain six-membered organic rings underwent ring contraction to give five-membered rings, with elimination of CO, under conditions of flash vacuum thermolysis.¹¹ For example, in this fashion, *o*-benzoquinones are converted to cyclopentadienones,^{12–14} 2-pyrone is transformed to furan,¹⁵ and hexafluorocyclohexadienones afford hexafluorocyclopentadiene.¹⁶ Coupling of this latent knowledge with subsequent reports of the preparation of ruthenium complexes containing the η^5 -oxocyclohexadienyl (η^5 -phenoxide) ligand^{17,18} suggested that analogous decarbonylations of the latter complexes to give η^5 -cyclopentadienyl ligands could be achieved, especially if they afforded stable metallocenes as the final organometallic product. Indeed, initial attempts were successful in affording the pentafluorocyclopentadienyl complexes **1**¹⁹ and **2**²⁰ via flash vacuum thermolysis (FVT) of the corresponding complexes **3** and **4**, Chart 1. The effects of perfluorination on the electronic properties of the cyclopentadienyl ligand were evaluated by measuring the gas-phase ionization free energy of **1**. It proved to be 18.5 kcal/mol higher than that of $[Ru(C_5Me_5)(C_5H_5)]$, confirming that perfluorination of a Cp ligand increases its electron-withdrawing ability, although the effects of σ -electron withdrawal are, not unexpectedly, strongly attenuated by π -donation from the fluorines.²¹ Similar conclusions result from a detailed comparison of the photoelectron spectra of **1** and its analogues $[Ru(C_5Me_5)(C_5H_5)]$ and $[Ru(C_5Me_5)(C_5Cl_5)]$.²²

In order to establish whether the effects of perfluorination of the cyclopentadienyl were additive and whether the specific location of fluorines on the ring made signi-

ficant differences, corresponding syntheses of isomerically pure partially fluorinated cyclopentadienyl rings were required. Here, we describe the selective preparation of the complete set of complexes containing partially fluorinated cyclopentadienyl rings and their oxocyclohexadienyl precursors. Studies confirming the approximate additivity of fluorine substituent effects in these new cyclopentadienyl compounds were recently published.²³

Results and Discussion

Partially Fluorinated (2–6- η^5 -Oxocyclohexadienyl)ruthenium Complexes $[RuCp^*(2-6-\eta^5-C_5F_{5-n}H_nCO)]$ ($n = 1-4$). The desired oxocyclohexadienyl complexes, $[RuCp^*(2-6-\eta^5-C_5F_{5-n}H_nCO)]$ $n = 1-4$, **5–11** (see Table 2), were synthesized similarly to their perfluorinated analogue **3**.¹⁹ Refluxing the ruthenium tetramer $[RuCp^*Cl]_4$ ($Cp^* = \eta^5-C_5Me_5$) in acetonitrile afforded, *in situ*, the $[RuCp^*(CH_3CN)_3]^+$ cation, which was subsequently treated with the Tl^+ salts of the appropriate commercially available fluorophenols to afford the corresponding partially fluorinated oxocyclohexadienyl complexes **5–11** in good yields.

All oxocyclohexadienyl products were characterized by IR, ¹H and ¹⁹F NMR spectra, and microanalysis; data are presented in Tables 1 and 2. The ¹H NMR spectra of **5–11** all exhibit a sharp singlet in the region 1.79–1.90 ppm for the Cp^* protons, with multiplets in the region 3.9–5.7 ppm corresponding to the protons of the fluoro-oxocyclohexadienyl ligands. Their ¹⁹F NMR spectra displayed the expected number of resonances in the appropriate ratio in the region from –160 to –194 ppm the significant upfield shift of the fluorine resonances from those of the corresponding free fluorophenols being consistent with η^5 coordination of the phenoxide ligands. The ¹⁹F–¹⁹F, ¹⁹F–¹H, ¹H–¹H coupling constants listed in Table 2 were obtained directly from the ¹H and ¹⁹F NMR spectra.

In confirmation of the 2–6- η^5 coordination mode of the phenoxide ligands, the IR spectra of **5–11** showed a strong C=O stretch. The position of this stretch is dependent upon the number and relative location of the fluorine atoms on the ligand. For the fully fluorinated ring in **3**, the observed value of ν_{CO} is 1620 cm^{-1} ,¹⁹ as expected, all values observed for **5–11** lie below this value and are consistent with a predominantly inductive electron-withdrawing effect of fluorine, exercised more potently at locations closer to the oxygen atom. The presence of two *ortho*-fluorines, in **5** and **9**, give the highest values of ν_{CO} (1582–1574 cm^{-1} ; Table 1), a single *ortho*-fluorine (in **6**, **7**, **8**, and **10**) affords values between 1541 and 1555 cm^{-1} , and no *ortho*-fluorines (in **11**) give the lowest value of 1534 cm^{-1} . In addition to C=O stretches, broad absorption bands around 3450 cm^{-1} attributable to water were also observed in the IR spectra of **6–11**. Consistent with this observation, the microanalysis data of the compounds (except for **7** and **8**) did not correlate to the calculated percentages of

(6) Hedberg, F. L.; Rosenberg, H. *J. Am. Chem. Soc.* **1970**, *92*, 3239.

(7) Hedberg, F. L.; Rosenberg, H. *J. Am. Chem. Soc.* **1973**, *95*, 870.

(8) Winter, C. H.; Han, Y.; Ostrander, R. L.; Rheingold, A. L. *Angew. Chem., Int. Engl.* **1993**, *32*, 1161.

(9) Paprott, G.; Seppelt, K. *J. Am. Chem. Soc.* **1984**, *106*, 4060.

(10) Paprott, G.; Lehmann, S.; Seppelt, K. *Chem. Ber.* **1988**, *121*, 727.

(11) For a discussion of this technique, see: Magrath, J.; Fowler, F. W. *Tetrahedron Lett.* **1988**, *29*, 2171 and references cited therein.

(12) DeJongh, D. C.; Van Fossen, R. Y.; Bourgeois, C. F. *Tetrahedron Lett.* **1967**, 271.

(13) DeJongh, D. C.; Brent, D. A.; Van Fossen, R. Y. *J. Org. Chem.* **1971**, *36*, 1469.

(14) Chapman, O. L.; McIntosh, C. L. *J. Chem. Soc., Chem. Commun.* **1971**, 770.

(15) Brent, D. A.; Hribar, J. D.; DeJongh, D. C. *J. Org. Chem.* **1970**, *35*, 135.

(16) Soelch, R. R.; Mauer, G. W.; Lemal, D. M. *J. Org. Chem.* **1985**, *50*, 5845.

(17) Bücken, K.; Koelle, U.; Pasch, R.; Ganter, B. *Organometallics* **1996**, *15*, 3095.

(18) Loren, S. D.; Campion, B. K.; Heyn, R. H.; Tilley, T. D.; Bursten, B. E.; Luth, K. W. *J. Am. Chem. Soc.* **1989**, *111*, 4712.

(19) Curnow, O. J.; Hughes, R. P. *J. Am. Chem. Soc.* **1992**, *114*, 5895.

(20) Hughes, R. P.; Zheng, X.; Rheingold, A. L.; Ostrander, R. L. *Organometallics* **1994**, *13*, 1567.

(21) Richardson, D. E.; Ryan, M. F.; Geiger, W. E.; Chin, T. T.; Hughes, R. P.; Curnow, O. J. *Organometallics* **1993**, *12*, 613.

(22) Lichtenberger, D. L.; Elkadi, Y.; Gruhn, N.; Hughes, R. P.; Curnow, O. J.; Zheng, X. *Organometallics* **1997**, *16*, 5209.

(23) Richardson, D. E.; Lang, L.; Eyley, J. R.; Zheng, X.; Morse, C. A.; Hughes, R. P. *Organometallics* **1997**, *16*, 149.

Chart 1

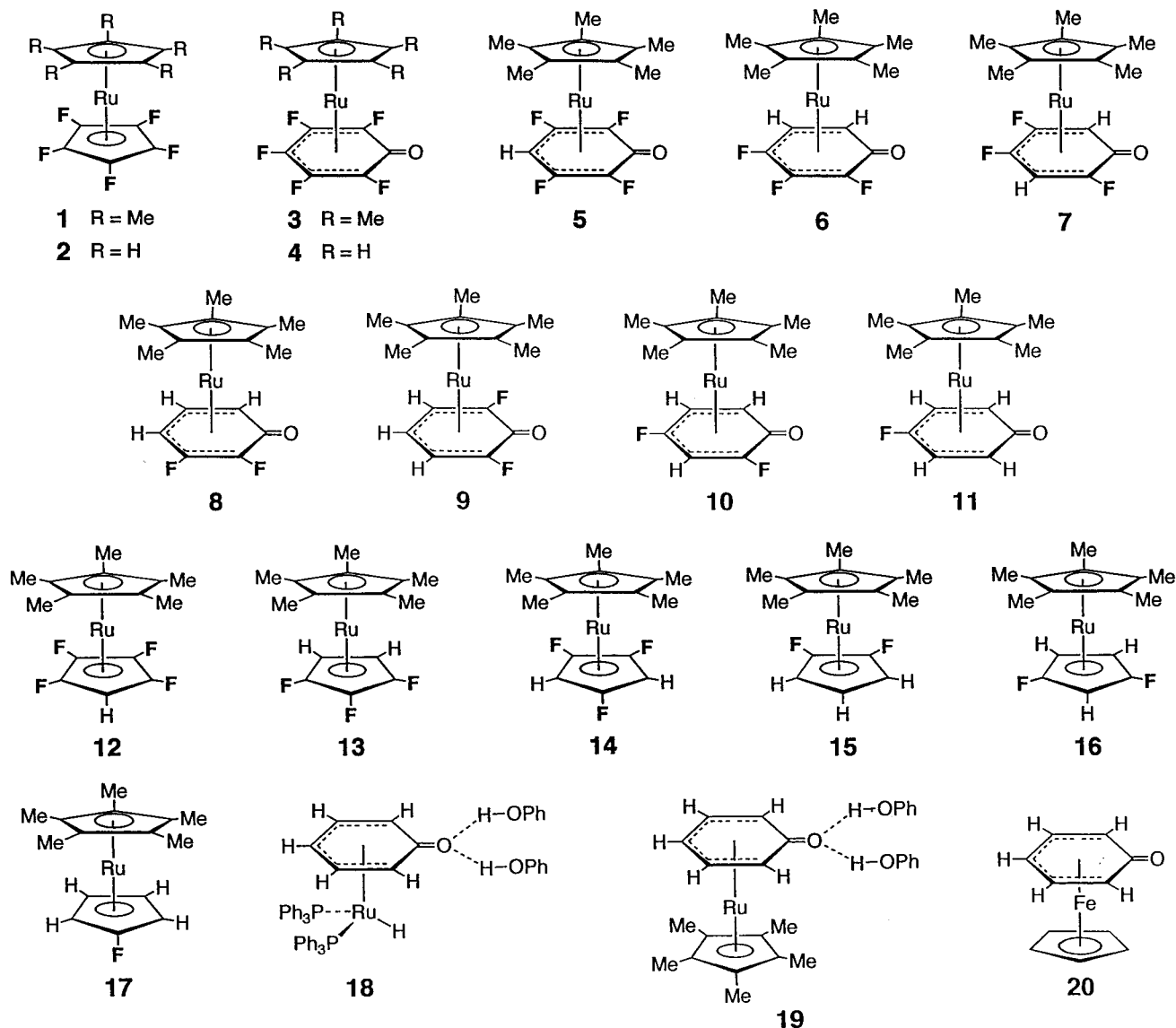


Table 1. IR and Microanalysis Data for 5–11

	microanalysis (%)				IR (cm ⁻¹)	
	calcd		found		$\nu_{C=O}$	ν_{O-H}
	C	H	C	H		
5	47.89	4.02	48.00	3.98	1582	
6	48.97 ^a	4.63 ^a	48.92	4.90	1548	3400–3500
7	50.13	4.47	50.09	4.40	1555	3400–3500
8	52.59	4.97	52.60	5.24	1543	3400–3500
9	51.33 ^a	5.12 ^a	51.71	4.94	1574	3400–3500
10	50.12 ^b	5.26 ^b	50.19	5.06	1541	3400–3500
11	52.59 ^b	5.89 ^b	52.82	5.84	1534	3300–3500

^a Calculated using 0.5 H₂O per formula unit. ^b Calculated using 1.0 H₂O per formula unit.

carbon and hydrogen unless one molecule (for **10**, **11**) or one-half (for **6**, **9**) of a molecule of water was added to their molecular formula. In the cases of **7** and **8**, special efforts were taken to exclude moisture during the purification process (see below). The ¹H NMR spectra of some complexes revealed broad resonances at about 3 ppm, confirmed as being due to hydroxylic protons by their disappearance upon addition of D₂O.

Since the compounds were synthesized in predried solvents under dry nitrogen, the water evident from the

IR spectra and microanalyses of **6**–**11** must have been incorporated after the samples had been prepared. However, on the basis of the assumption that they were as air stable in the solid state as the perfluorinated analogue **3**, compounds **5**, **6**, and **9**–**11** were exposed to the air in the subsequent purification (sublimation, chromatography) and characterization processes. The water affinity of **6**–**11** likely originates from the hydrogen-bonding tendency of the oxygen atom in the oxocyclohexadienyl ligand. Indeed, the hydrogen-bonding ability of the oxygen atom in analogous oxocyclohexadienyl ligands is well-established. X-ray crystallographic studies have demonstrated that complexes **18** and **19** show this hydrogen-bonding ability to phenol,^{24,25} and NMR studies have also illustrated a 1:1 solution interaction between D₂O and a series of oxocyclohexadienyliron complexes like **20**.²⁶ The number of water

(24) Chaudret, B.; He, X.; Huang, Y. *J. Chem. Soc., Chem. Commun.* **1989**, 1844. Koelle, U.; Wang, M. H.; Raabe, G. *Organometallics* **1991**, *10*, 2573.

(25) Cole-Hamilton, D. J.; Young, R. J.; Wilkinson, G. *J. Chem. Soc., Dalton Trans.* **1976**, 1995.

(26) Piorko, A.; Zhang, C. H.; Reid, R. S.; Lee, C. C.; Sutherland, R. G. *J. Organomet. Chem.* **1990**, *395*, 293.

Table 2. ^1H and ^{19}F NMR Spectral Data for **5–11**^a

	δ_{F}	δ_{H}		J_{FF}	J_{HF}	J_{HH}
		Cp*(s) other	$\text{OC}_6\text{F}_{5-n}\text{H}_n$			
	-170.5 (m, 2F) -188.0 (m, 2F)	1.90	5.46 (bs)			
	-180.1 (dd, F ₂) -185.8 (td, F ₁) -191.9 (ddd, F ₃)	1.85 2.7 (s, H ₂ O)	4.67 (ddd, H ₁) 5.22 (dd, H ₂)	$J_{\text{F}_1\text{F}_2} = 37.4$ $J_{\text{F}_1\text{F}_3} = 8.3$ $J_{\text{F}_2\text{F}_3} = 38.7$	$J_{\text{H}_1\text{F}_3} = 4.3$ $J_{\text{H}_2\text{F}_1} = 2.1$ $J_{\text{H}_1\text{F}_2}$ or $J_{\text{H}_1\text{F}_1} = 1.1$	$J_{\text{H}_1\text{H}_2} = 6.3$
	-168.2 (ddd, F ₂) -172.4 (d, F ₁) -180.4 (d, F ₃)	1.83	5.15 (bs, H ₂) 5.69 (t, H ₁)	$J_{\text{F}_1\text{F}_2} = 10$ $J_{\text{F}_1\text{F}_3} = 0$ $J_{\text{F}_2\text{F}_3} = 35$	$J_{\text{H}_1\text{F}_2} = 2.2$	
	-170.3 (d, F ₂) -193.6 (d, F ₁)	1.88 2.8 (s, H ₂ O)	4.8 (m, 2H) 5.11 (m, 1H)	$J_{\text{F}_1\text{F}_2} = 35.2$		
	-169.7 (bs)	1.87	4.69 (tt, H ₂) 5.25 (dt, H ₁)		$(J_{\text{H}_1\text{F}_1})_{\text{app}} = 2.7$ $J_{\text{H}_2\text{F}_1} = 1.8$	$J_{\text{H}_1\text{H}_2} = 5.4$
	-162.4 (bs, F ₁) -171.3 (bs, F ₂)	1.79 3.0 (bs, H ₂ O)	4.12 (dt, H ₂) 5.12 (dq, H ₃) 5.58 (dd, H ₁)		$J_{\text{H}_2\text{F}_2} = 6$ $J_{\text{H}_3\text{F}_2} = 1.5$ $J_{\text{H}_3\text{F}_1} = 1.5$	$J_{\text{H}_1\text{H}_2} = 2$ $J_{\text{H}_1\text{H}_3} = 1$ $J_{\text{H}_2\text{H}_3} = 6$
	-162.9 (bs)	1.86 3.0 (bs, H ₂ O)	4.64 (m, 2H) 5.26 (m, 2H)			

^a Solvent: CDCl_3 ; Units: δ in ppm; J in hertz. For other general information on the NMR experiments, see the Experimental Section. Subscript app stands for apparent bs for broad singlet.

molecules associated with **6**, **9**, **10**, and **11**, as indicated by microanalysis data, correlates inversely to $\nu_{\text{C}=\text{O}}$ and also to the number and relative position of F substituents on the fluorooxocyclohexadienyl ligand. If the hydrogen-bonding capability of the oxocyclohexadienyl ligand reflects the amount of negative charge residing on the oxygen atom, F substituents will clearly compete for the negative charge of the ligand and reduce the hydrogen-bonding ability of the oxygen. More F substituents closer to oxygen lead to a less anionic oxygen atom, a stronger $\text{C}=\text{O}$ bond, and a lower tendency for the oxygen to form hydrogen bonds.

Partially Fluorinated Cyclopentadienylruthenium Complexes $[\text{RuCp}^*(\eta^5\text{-C}_5\text{F}_{5-n}\text{H}_n)]$ ($n = 1-4$). In a manner analogous to the FVT conversion of the perfluorinated precursors **3** and **4** to their $\eta^5\text{-C}_5\text{F}_5$ complexes **1**¹⁹ and **2**,²⁰ each of the partially fluorinated precursors **5–11** afforded the partially fluorinated cyclopentadienylruthenium complexes **12–17** (see Table 3). As observed in the FVT of **3** and **4**, thin films of a black material were formed in the quartz pyrolysis tubes. This material was characterized by qualitative X-ray microanalysis and found to be composed of mostly Ru and C and traces of O and Si. Yields and conversions were variable and difficult to control in a reproducible fashion, making this a less than optimum synthetic method. For example, FVT of the tetrafluoro complex

5 cleanly afforded **12** in 42% yield, whereas FVT of monofluorinated **11** afforded **17** in only 9% yield. Yields and conversions were not optimized, and details of the furnace temperatures, yields, and conversions are presented in the Experimental Section. All thermolysis reactions proceeded cleanly to give the fluorine substituent pattern on the resultant cyclopentadienyl ring, consistent with that expected from the precursor complex(es). In some cases, traces of isomeric impurities and complexes containing fewer fluorines than expected could be observed by ^{19}F NMR spectroscopy at levels between 1–2%; in all cases, these impurities could be traced back to impurities in the starting phenols, which were purchased commercially and not purified before use. We conclude that in the actual thermolysis experiments no rearrangements or elimination reaction occur to any significant extent.

The partially fluorinated cyclopentadienyl products **12–17** were characterized by ^1H , ^{19}F , and $^{13}\text{C}\{^1\text{H}\}$ NMR spectra (Table 3). The molecular formulas of **12–14** were confirmed by microanalysis. The ^1H NMR spectra all show a Cp* proton resonance in the region from 1.88 to 1.74 ppm; the corresponding resonances in **1** and $[\text{RuCp}^*(\text{C}_5\text{H}_5)]$ appear at 1.68 and 1.90 ppm, respectively. The resonances corresponding to the protons on the fluorocyclopentadienyl ligands appear in the region 3.51–4.43 ppm. All of the ^{19}F NMR spectra of **12–17**

Table 3. 1H , ^{19}F , and $^{13}C\{^1H\}$ NMR data for 12–17^a

	δ_H		δ_F	δ_C			$^1J_{CF}$	$^2J_{CF}$	$^3J_{CF}$
	Cp*	Cp ^F		Me(Cp*)	ring(Cp*)	ring(Cp ^F)			
 12	1.74 (s)	3.74 (tt, H ₁)	-203.5 (td, F ₂) -214.0 (td, F ₃)	11.01 (s)	90.67 (s)	43.97 (t, C ₁) 108.38 (dm) 111.51 (dm)	$J_{C_2F_2} = 285$ $J_{C_3F_3} = 295$	$J_{C_1F_2} = 16.6$	
	$J_{F_2F_3}^{app} = 25.5$ $J_{H_1F_2} = 5.7$ $J_{H_1F_3} = 2.3$								
 13	1.80 (s)	3.51 (td, H ₃)	-215.3 (tt, F ₁) -201.1 (dt, F ₂)	11.33	89.16	112.36 (dt, C ₁) 117.88 (ddd, C ₂) 51.15 (~dd, C ₃)	$J_{C_1F_1} = 274.1$ $J_{C_2F_2} = 276.2$	$J_{C_1F_2} = 13.8$ $J_{C_2F_1} = 12.2$	$J_{C_2F_2} = 1.5$
	$J_{F_2H_3}^{app} = 2.6$ $J_{F_1F_2} = 23.4$ $J_{F_1H_3} = 1.0$								
 14	1.79 (s)	4.09 (dt, H ₂)	-190.2 (tt, F ₁) -203.4 (dt, F ₂)	11.35	87.09	119.8 (dt, C ₁) 48.4 (ddd, C ₂) 117.0 (ddd, C ₃)	$J_{C_1F_1} = 279.8$ $J_{C_3F_3} = 279.7$	$J_{C_3F_3'} = 15.9$ $J_{C_2F_1} = 17.4$ $J_{C_2F_3} = 8.7$ $J_{C_2F_3'} = 6.3$	$J_{C_1F_3} = 2.0$ $J_{C_3F_1} = 3.2$
	$J_{H_2H_3}^{app} = 3.0$ $J_{F_1F_3} = 18.7$ $J_{F_1H_2} = 4.1$								
 15	1.85 (s)	3.27 (t, H ₁) 4.96(dt, H ₂)	-204.5 (t, F ₃)	11.65	87.68	59.05 (t, C ₁) 57.72 (~dd, C ₂) 122.78 (dd, C ₃)	$J_{C_3F_3} = 271.7$	$J_{C_3F_3'} = 14.6$ $J_{C_2F_3} = 8.7$	$J_{C_2F_3'} = 5.9$ $J_{C_1F_3} = 2.3$
	$J_{H_2H_3}^{app} = 2.3$ $J_{H_1H_2} = 2.8$								
 16	1.84 (s)	4.43 (tt, H ₁) 3.85 (~dt, H ₃)	-189.1 (-dt, F ₂)	11.7	87.55	51.82 (t, C ₁) 127.30 (dd, C ₂) 56.66 (~dd, C ₃)	$J_{C_2F_2} = 273.3$	$J_{C_1F_2} = 16.5$ $J_{C_3F_2} = 11.6$	$J_{C_2F_2'} = 5.3$ $J_{C_3F_2} = 7.3$
	$J_{F_2H_3}^{app} = 1.8$ $J_{H_1H_3} = 1.3$ $J_{H_1F_2} = 4.1$								
 17	1.88 (s)	4.28 (dt, H ₂) 3.73 (t, H ₃)	-192.3 (t, F ₁)	12.08	86.27	134.17 (d, C ₁) 61.8 (d, C ₂) 66.8 (d, C ₃)	$J_{C_1F_1} = 266.8$	$J_{C_2F_1} = 16.0$	$J_{C_3F_1} = 3.6$
	$J_{H_2H_3}^{app} = 1.8$ $J_{F_1H_2} = 3.5$								

^a $^{13}C\{^1H\}$ NMR spectra were recorded in $CDCl_3$, 1H and ^{19}F NMR spectra in C_6D_6 . Units: δ in ppm; J in hertz. For other general information on NMR experiments, see the Experimental Section. Subscript app stands for apparent ~dd for approximate doublet of doublets, and Cp^F for the fluorinated Cp ligand.

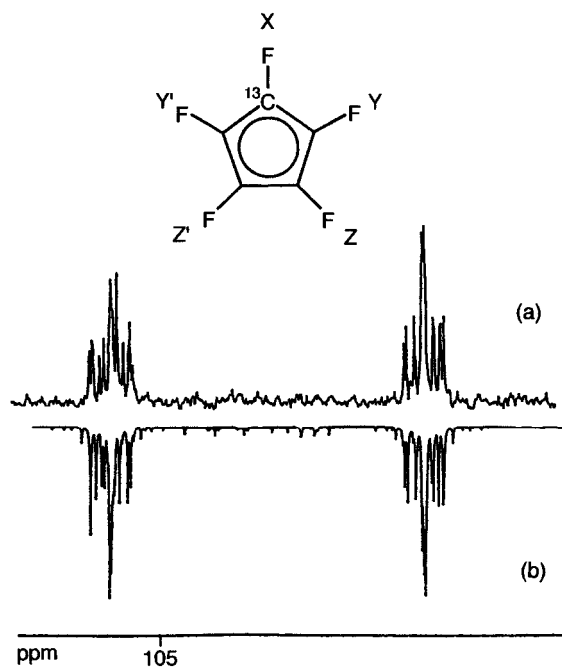


Figure 1. (a) Experimental and (b) simulated ^{13}C NMR resonance for the pentafluorocyclopentadienyl ring carbon of **1**. Simulated as an AXYY'ZZ' spin system (see labeling scheme) with $J_{\text{AX}} = 295.00$, $J_{\text{AY}} = J_{\text{AY}'} = -16.00$, $J_{\text{AZ}} = J_{\text{AZ}'} = 2.00$, $J_{\text{XY}} = J_{\text{XY}'} = 23.00$, $J_{\text{XZ}} = J_{\text{XZ}'} = 19.00$, $J_{\text{YY}'} = 19.00$, $J_{\text{ZZ}'} = 23.00$, $J_{\text{YZ}} = J_{\text{YZ}'} = 23.00$, $J_{\text{YZ}'} = J_{\text{YZ}'} = 19.00$; $\delta(^{13}\text{C}) = 7777.50$, $\delta_{\text{FX}} = -59896.00$, $\delta_{\text{FY}} = \delta_{\text{FY}'} = -59826.00$ Hz, $\delta_{\text{FZ}} = \delta_{\text{FZ}'} = -59820.00$ (all values in hertz).

display the expected number of resonances in the right ratios in the region from -189 to -216 ppm. By way of comparison, the fluorine chemical shifts of **1** and **2** are -213.2 and -206.9 ppm, respectively. The chemical shifts of the fluorine substituents in **12–17** and in their Cp^* analogue **1** are almost independent of the total number of fluorines but do depend on their relative positions: a fluorine vicinally adjacent to no other fluorines has a chemical shift of about -190 ppm; a fluorine adjacent to one other fluorine has a chemical shift of around -204 ppm; and a fluorine sandwiched between two other fluorines has a chemical shift of approximately -214 ppm. The $^{13}\text{C}\{^1\text{H}\}$ NMR spectra of **12–17** all exhibit two singlets in the region $11–12$ and $86–91$ ppm corresponding, respectively, to the ring carbon and methyl substituents of the Cp^* ligand. Resonances due to the fluorinated cyclopentadienyl ligands appear in two separate regions: $108–135$ ppm for carbon atoms bearing a F substituent and $44–66$ ppm for the unsubstituted carbon atoms. All $^{13}\text{C}-^{19}\text{F}$, $^{19}\text{F}-^{19}\text{F}$, $^{19}\text{F}-^1\text{H}$, and $^1\text{H}-^1\text{H}$ coupling constants listed in Table 3 were obtained directly from the spectra.

The long range $^{19}\text{F}-^{13}\text{C}$ coupling constants for the partially fluorinated cyclopentadienyl ligands provided useful reference data to help simulate the ^{13}C NMR spectrum of the originally reported pentafluorocyclopentadienyl complex **1**. In the initial report,¹⁹ the carbon resonance of the fluorinated ring was reported as a broad doublet, with only the value of $^1J_{\text{CF}}$ being readily apparent. Under higher resolution conditions, a much more complex pattern emerged, as shown in Figure 1. This was eventually simulated as an AXYY'ZZ' spin system (labeling as shown in Figure 1) by

recognizing that the presence of a single ^{13}C nucleus in the $\eta^5\text{-C}_5\text{F}_5$ ring should lead to different chemical shift perturbations for the different fluorines in the ring.²⁷ The successful simulation data are presented in Figure 1.

The solid-state structures of two of these partially fluorinated metallocenes, **15** and **17**, were confirmed by X-ray crystallographic studies. Details of the crystallographic determinations are provided in Table 4. The ORTEP diagram of **15** is shown in Figure 2, and a schematic diagram showing relevant bond lengths within the cyclopentadienyl rings is shown in Figure 3. The two C_5 rings are eclipsed, consistent with the structures of ruthenocene²⁸ and $[\text{Ru}(\text{C}_5\text{Me}_5)(\text{C}_5\text{H}_5)]$.²⁹ Unlike ruthenocene itself,²⁸ the two rings in **15** are not parallel. Examination of the $\text{Ru}-\text{C}$ bond distances for the difluorocyclopentadienyl ligand in **15** shows the three $\text{Ru}-\text{C}(\text{H})$ distances ($2.186(9)$, $2.189(10)$, and $2.197(11)$ Å) to be identical to the average $\text{Ru}-\text{C}(\text{H})$ distance ($2.191(7)$ Å) in ruthenocene or in $[\text{Ru}(\text{C}_5\text{Me}_5)(\text{C}_5\text{H}_5)]$ ($2.190(5)$ Å). However, one of the two $\text{Ru}-\text{C}(\text{F})$ distances in **15** is considerably shorter ($2.133(11)$ Å) and the other slightly shorter ($2.164(10)$ Å). Correspondingly, the five $\text{Ru}-\text{C}(\text{Me})$ distances show a significant inequivalence, with the two carbon atoms eclipsing the fluorine bearing carbon atoms being significantly closer ($2.122(13)$ and $2.123(13)$ Å) to the metal center. The overall result is that the metallocene rings become slightly canted. The shorter $\text{Ru}-\text{C}(\text{F})$ distances are consistent with, although less significant than, the shortening of $\text{M}-\text{C}$ distances in unsaturated fluorocarbon ligands such as $\eta^2\text{-C}_2\text{F}_4$ ³⁰ and $\eta^5\text{-C}_5\text{F}_5$ ²⁰ as compared to their hydrocarbon analogues.¹

The structure of **17** is similar to that of ruthenocene, although disorder problems thwarted a more detailed comparison. The fluorine atom in **17** was located at three disordered positions with a $56\text{--}28\text{--}16\%$ distribution, the Cp^* ligand was treated as a rigid body disordered in two rotational positions with a $70\text{--}30\%$ distribution. An ORTEP diagram illustrating the principal occupancy fluorine site is provided in Figure 4. In view of this disorder, a detailed structural analysis is not presented.

Conclusions

The FVT reaction of a series of partially fluorinated oxocyclohexadienyl complexes does provide a selective method for the synthesis of partially fluorinated cyclopentadienyl complexes, and the complete set of partially fluorinated cyclopentadienyl rings has thereby been obtained. While the method is not as high yield as could be desired, it appears to be the only method currently available for synthesis of selectively fluorinated ligands of this type. The selectively fluorinated complexes thus prepared have been subjected to a study of their gas-phase ionization energetics, the results of which have been published separately.²³ The series of $^{13}\text{C}-^{19}\text{F}$ coupling constants for fluorocyclopentadienyl ligands

(27) We are grateful to Prof. David M. Lemal for this suggestion.

(28) Seiler, P.; Dunitz, J. *Acta Crystallogr.* **1980**, *B36*, 2946.

(29) Zanin, I. E.; Antipin, M. Y.; Struchkov, Y. T. *Kristallografiya* **1991**, *36*, 420.

(30) Guggenberger, L. J.; Cramer, R. *J. Am. Chem. Soc.* **1972**, *94*, 3779.

Table 4. Crystallographic Data for 15 and 17

	15	17
(a) Crystal Parameters		
formula	$C_{15}H_{18}F_2Ru$	$C_{15}H_{19}FRu$
fw	337.4	319.4
cryst syst	monoclinic	monoclinic
space group	$P2_1/n$	$P2_1/n$
<i>a</i> , Å	8.376(2)	8.320(4)
<i>b</i> , Å	14.191(4)	13.976(5)
<i>c</i> , Å	12.013(5)	11.948(6)
<i>b</i> , deg	93.20(3)	92.37(3)
<i>V</i> , Å ³	1425.8(8)	1388.1(11)
<i>Z</i>	4	4
cryst dimens, mm	0.24 × 0.38 × 0.60	0.40 × 0.40 × 0.40
cryst color	yellow	yellow
<i>D</i> (calcd), g cm ³	1.572	1.528
μ (Mo K α), cm ⁻¹	11.02	11.17
temp, K	296	293
(b) Data Collection		
diffractometer		Siemens P4
monochromator		graphite
radiation		Mo K α ($\lambda = 0.71073$ Å)
2 θ scan range, deg	4–52	4–50
data collected (<i>h, k, l</i>)	±10, +17, +14	±9, +16, +14
no. of rflns collected	2935	2551
no. of indep rflns	2802	2433
no. of indep obsd rflns, $F_o > n\sigma(F_o)$	1874 (<i>n</i> = 5)	1941 (<i>n</i> = 4)
std rflns std/rfln	3/197	3/197
variance in stds, %	4	3
(c) Refinement		
<i>R</i> (<i>F</i>), %	6.71 ^a	4.11 ^b
<i>R</i> (<i>wF</i>), %	9.54 ^a	11.94 ^b
Δ/σ (max)	0.123	0.328
$\Delta(\rho)$, e Å ⁻³	2.14	1.025
<i>N</i> _o / <i>N</i> _v	11.5	11.75
GOF	1.74	1.12

^a Quantity minimized: $\sum w(F_o - F_c)^2$. ^b Quantity minimized: $\sum [w(F_o^2 - F_c^2)^2] / \sum [w(F_o^2)^2]^{1/2}$.

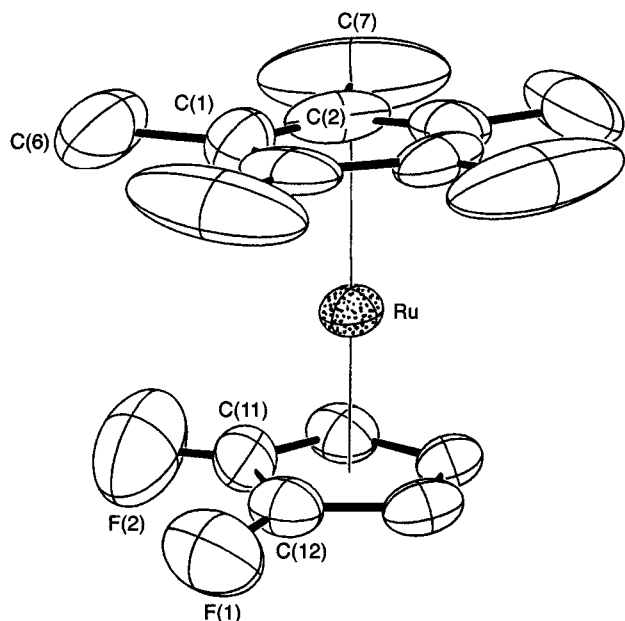


Figure 2. ORTEP diagram with labeling scheme for 15. Thermal ellipsoids are drawn at 30% probability.

proved to be invaluable reference data in facilitating a simulation of the ¹³C NMR resonance of the pentafluorocyclopentadienyl ring in 1.

Experimental Section

General Considerations. All reactions except FVT experiments were performed in oven-dried glassware, using standard

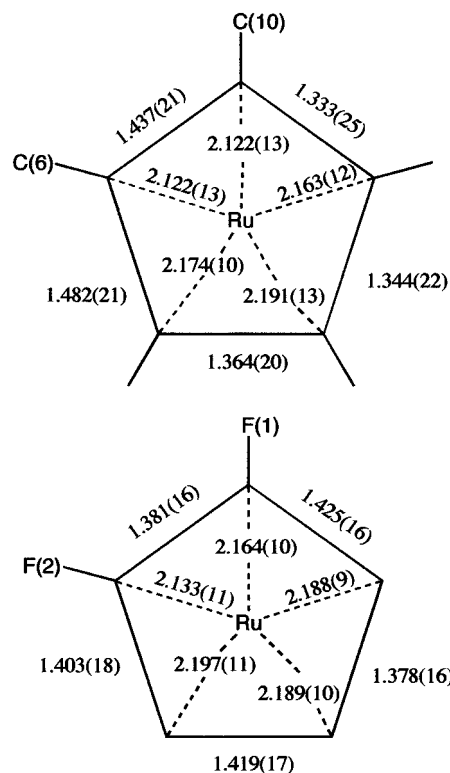


Figure 3. Key bond distances (Å) in complex 15.

Schlenk techniques, under an atmosphere of nitrogen which had been deoxygenated over BASF catalyst and dried over Aqasorb. All solvents were obtained from Fisher Scientific and distilled under nitrogen over one of the following drying

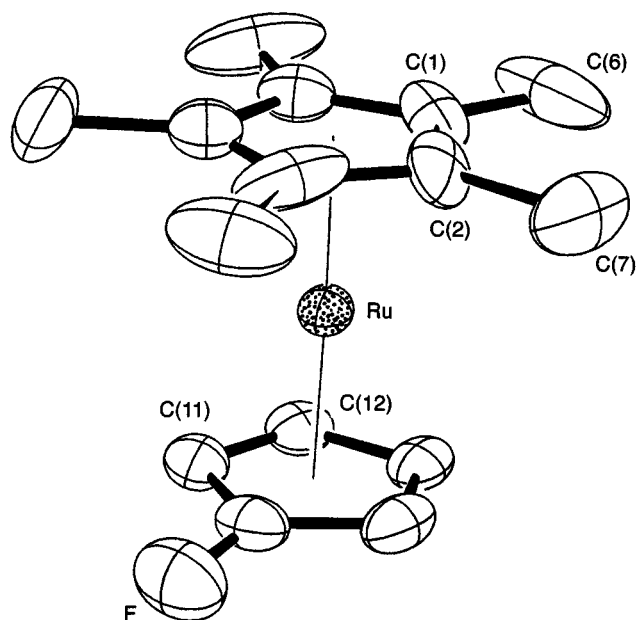


Figure 4. ORTEP diagram with labeling scheme for **17**. Thermal ellipsoids are drawn at 30% probability. The fluorine atom was located at three disordered positions with 56–28–16% distribution; only the 56% occupancy site is shown.

agents: THF and diethyl ether over K/benzophenone; methylene chloride, petroleum ether and acetonitrile over CaH_2 . Aromatic and unsaturated components of 35–65 °C petroleum ether were removed before distillation by prolonged stirring over concentrated H_2SO_4 followed by washing with 10% aqueous solution of KOH. Infrared spectra were recorded on a Perkin-Elmer model 1600 FT-IR spectrophotometer. Microanalyses were performed by Schwarzkopf Microanalytical Laboratory (Woodside, NY). ^1H (300 MHz), $^{13}\text{C}\{^1\text{H}\}$ (75 MHz), and ^{19}F (282 MHz) NMR spectra were recorded on a Varian XL-300 spectrometer or a Varian Unity Plus 300 system in the solvent indicated. All ^{19}F NMR chemical shifts are reported as ppm upfield from CFCl_3 , while ^1H and $^{13}\text{C}\{^1\text{H}\}$ shifts are reported as ppm downfield of internal TMS and are referenced to the solvent peak. Coupling constants are reported in hertz and obtained either directly from the first-order spectra or from computer simulation of the second-order spectra.

$\text{RuCl}_3 \cdot 3\text{H}_2\text{O}$ was obtained from Johnson-Matthey Aesar/Alfa. Thallium(I) ethoxide was purchased from Strem. Fluorophenols were purchased from Aldrich. $[\text{RuCp}^*\text{Cl}]_4$ was prepared following the literature procedure.³¹

The FVT experiments were performed using a model 55347 moldatherm hinged tube furnace (three continuous hot zones, maximum heating length = 24 in., maximum usable o.d. tube = 3 in.) connected with a model 58434 control console, both purchased from Lindberg/Blue M, a unit of General Signal. Qualitative X-ray microanalysis was performed at the Rippl Electron Microscope Facility of Dartmouth College, on a Zeiss DSM 962 scanning electron microscope at a 15 kV accelerating voltage, using a link eXL analysis system and Pentafet UTW Si(Li) X-ray detector, with a spectral resolution of 133 eV at 5.9 KeV.

Syntheses of Thallium Phenoxides. All of the thallium phenoxide salts were prepared by the following general procedure. Thallium(I) ethoxide (0.4 mL, 5.6 mmol) was syringed into a solution of the appropriate fluorophenol (5.7 mmol) in petroleum ether (45–50 mL) under nitrogen. The resultant white precipitate was filtered in air and rinsed with

petroleum ether. Yields were typically 90–100%. These complexes were used for the preparation of **5–11** without being further characterized.

Syntheses of $[\text{RuCp}^*(2-6-\eta^5\text{-C}_5\text{F}_5\text{-}n\text{H}_n\text{CO})]$ ($n = 1-4$). Compounds **5–11** were prepared following a modified procedure for the preparation of pentafluorocyclohexadienyl complex **3**.¹⁹ Tables 1 and 2 in the main text contain the microanalysis, IR, and ^1H and ^{19}F NMR spectra data of **5–11**. Microanalysis samples were purified by sublimation. The following general procedure is outlined for **5**:

An deep orange acetonitrile solution of $[\text{RuCp}^*(\text{CH}_3\text{CN})_3]\text{-Cl}$ was obtained by refluxing an acetonitrile (100 mL) solution of $[\text{RuCp}^*\text{Cl}]_4$ (0.75 g, 2.76 mmol Ru) for 3 h. Previously prepared $[\text{Ti}(2,3,5,6\text{-OC}_6\text{F}_4\text{H})]$ (1.02 g, 2.75 mmol) was added, and the resultant mixture was refluxed overnight to give a light yellow solution with a white precipitate (TlCl). The mixture was filtered, the solvent was removed *in vacuo*, and the remaining residue was extracted with methylene chloride (65 mL). Evaporation of the extract afforded a tan solid, which was subsequently sublimed (160 °C, 10^{-2} Torr) to yield a white solid **5** (0.64 g, 1.59 mmol; 58%).

Similarly prepared were **6** (87%), **7** (74%), **8** (75%), **9** (46%), **10** (49%), and **11** (39%).

Syntheses of $[\text{RuCp}^*(\eta^5\text{-C}_5\text{F}_5\text{-}n\text{H}_n)]$ ($n = 1-4$). All percentage yields of the products are based on the amounts of the precursors consumed in the cases of less than 100% conversion. ^1H , ^{19}F , and $^{13}\text{C}\{^1\text{H}\}$ NMR spectral data of **12** are provided in Table 3. A typical procedure for the conversion of **5** to **12** follows:

Compound **5** (0.13 g, 0.31 mmol) was evaporated under dynamic vacuum (10^{-4} Torr) and mild heating (120 °C) at the sealed end of a quartz tube (4 ft in length \times 0.95 cm i.d.) and was allowed to pass through the tube with all three zones set at 710 °C. A shiny black film was deposited on the inside wall of the highly heated part of the tube (see text). Solids condensed at ambient temperature in the exit tube and were rinsed from the tube with methylene chloride. ^{19}F NMR spectra of the crude extracts in CDCl_3 showed the resonances of **12** and traces of **5**. Purification by sublimation (105–110 °C, 10^{-2} Torr) afforded a pale yellow solid **12** (0.05 g, 0.13 mmol) in 42% yield. Anal. Calcd for $\text{C}_{15}\text{H}_{16}\text{F}_4\text{Ru}$: C, 50.50; H, 4.82. Found: C, 50.40; H, 4.91.

When the temperature of the furnace was set at 690 °C (all three zones), conversion was 97%; at 690, 680, and 650 °C, conversion was 96%; at 680 °C (all three zones), conversion was 74%; at 650, 650, and 630 °C, conversion was 78%; at 610, 570, and 487 °C, conversion was about 10%.

In a similar fashion, the vapor of compound **6** (0.10 g, 0.25 mmol) was allowed to pass through the hot zone (670 ± 10 °C, 0.95 cm i.d. \times 35 cm in length). The crude product was purified by sublimation (70–90 °C, 10^{-2} Torr) to give a white solid, **13** (0.03 g, 0.08 mmol, 32%). Anal. Calcd for $\text{C}_{15}\text{H}_{17}\text{F}_3\text{-Ru}$: C, 50.70; H, 4.82. Found: C, 50.81; H, 4.98. Under the same reaction conditions used for the preparation of **13**, except for a decreased furnace temperature (630 °C), **7** (0.11 g, 0.29 mmol) was converted to a yellowish product mixture from which **14** (0.06 g, 0.17 mmol) was isolated in 59% yield by chromatography (1 cm i.d. \times 1 cm in length silica gel column, eluting with a mixture of 1 mL of methylene chloride and 7 mL of petroleum ether). In a second experiment, when the furnace temperature was maintained at 605 °C, the conversion was 85%. Anal. Calcd for $\text{C}_{15}\text{H}_{17}\text{F}_3\text{Ru}$: C, 50.70; H, 4.82. Found: C, 50.40; H, 4.91.

In similar fashion, compound **8** (0.18 g, 0.50 mmol) was evaporated under a dynamic vacuum (10^{-4} Torr) at the sealed end of a quartz tube (4 ft in length \times 0.95 cm i.d.), and was passed through the three hot zones of the furnace set at 750, 750, and 740 °C, respectively. The crude product was purified by gradient sublimation (vacuum = 10^{-3} Torr; Pyrex tubing = 0.5 cm i.d. \times 65 cm, gradient = 60 °C to room temperature) to give pure **15** (0.011 g, 0.03 mmol, 6%). Similarly, precursor

(31) Fagan, P. J.; Ward, M. D.; Calabrese, J. C. *J. Am. Chem. Soc.* **1989**, *111*, 1698.

9 (0.20 g, 0.56 mmol) was subjected to FVT (710 °C, 10^{-4} Torr, 0.48 cm i.d. \times 60 cm in length) under conditions of 88% conversion to afford **15** (0.081 g, 0.24 mmol, 38%).

In an analogous fashion, complex **10** (0.19 g, 0.53 mmol) was pyrolyzed at 10^{-4} Torr, zone temperatures of 770, 770, and 760 °C. Purification by gradient sublimation (4×10^{-4} Torr, 0.5 cm i.d. \times 65 cm in length, Pyrex tubing, 30–60 °C) and subsequent chromatography (1.5 cm in length \times 0.5 cm i.d. Al_2O_3 column, 50 mL of petroleum ether as eluate) afforded **16** (0.02 g, 0.06 mmol, 10%).

The FVT reaction of **11** (0.25 g, 0.69 mmol) was conducted in an analogous fashion, except that the temperature of the furnace had to be raised to 795, 795, and 785 °C to achieve 100% conversion. Purification of the crude product by chromatography (10 cm in length \times 1.5 cm i.d. Al_2O_3 column, petroleum ether as eluate) followed by gradient sublimation (4×10^{-4} Torr, 0.5 cm i.d. \times 65 cm in length, Pyrex tubing, 60–20 °C gradient) afforded **17** (0.018 g, 0.06 mmol, 9%).

Crystallographic Studies of 15 and 17. Details of the crystallographic determinations are given in Table 4. Suitable crystals were selected and mounted with epoxy cement to glass fibers. The unit-cell parameters were obtained by the least squares refinement of the angular settings of 24 reflections ($20^\circ \leq 2\theta \leq 25^\circ$). The systematic absence in the diffraction data for the isomorphous **15** and **17** are uniquely consistent for space group $P2_1/n$. The structures were solved using direct methods, completed by subsequent difference Fourier syntheses, and refined by full-matrix least-squares procedures. All non-hydrogen atoms were refined with anisotropic displace-

ment coefficients. Hydrogen atoms were treated as idealized contributions in **15** and ignored in **17**. The pentamethylcyclopentadienyl ring in **17** was treated as a rigid body disordered in two rotational positions with a 70–30% distribution. The fluorine atom in **17** was located at three disordered positions with a 56–28–16% distribution.

All software and sources of the scattering factors are contained in either the SHELXTL-92 (Gamma Test), SHELXTL (5.1), or SHELXTL PLUS (4.2) program libraries (G. Sheldrick, Siemens XRD, Madison, WI).

Acknowledgment. R.P.H. acknowledges support of this research by the National Science Foundation and the Petroleum Research Fund, administered by the American Chemical Society. A generous loan of $RuCl_3 \cdot 3H_2O$ from Johnson-Matthey \AE sar/Alfa is also gratefully acknowledged. The assistance of Charles P. Daghljan in obtaining X-ray microanalyses at the Rippel Electron Microscope Facility at Dartmouth College is also acknowledged.

Supporting Information Available: Tables of the X-ray structure determinations, atomic coordinates and anisotropic thermal parameters, bond lengths and bond angles, anisotropic displacement parameters, and hydrogen atom coordinates for **15** and **16** (19 pages). Ordering information is given on any current masthead page.

OM970775P